LIX1L promotes EMT and EGFR-TKIs resistance via nucleolin-mediated ribosomal RNA synthesis in NSCLC

Minglei Li
Hebei Medical University
Jiaxi Zhang
Hebei Medical University
Xue Meng
Hebei Medical University
Bei Liu
Hebei Medical University
Shelly Xie
Hebei Medical University
Fang Liu
Hebei Medical University
Demin Yao
Hebei Medical University
Jingguo Zhang
Hebei Medical University
Haitao Shen
Hebei Medical University
Lingxiao Xing (xinglingxiao@hotmail.com)
Hebei Medical University

Article

Keywords: LIX1L, nucleolin, ribosomal RNA synthesis, EMT, EGFR-TKIs resistance, NSCLC

Posted Date: June 21st, 2022

DOI: https://doi.org/10.21203/rs.3.rs-1749938/v1

Abstract

Limb expression 1-like protein (LIX1L) might be an RNA binding protein involved in post-transcriptional regulation. However, little is known regarding the biological function and mechanism of LIX1L in cancer cells. Here we demonstrate a clear correlation between LIX1L expression and EMT markers in 81 NSCLC tissues and TCGA database, suggesting that LIX1L is a mesenchymal marker. Besides, LIX1L expression is obviously elevated in TGFβ1-induced EMT NSCLC cells, and enhances cell migration, invasion, anoikis resistance, EGFR-TKIs resistance and proliferation. Interestingly, the increased LIX1L expression prominently localizes to the nucleoli, where it physically interacts with the key ribosome biogenesis regulator NCL protein, inducing rRNA synthesis in EMT NSCLC cells. NCL knockdown or inhibition of rRNA synthesis reverses the enhanced EMT functions and proliferation ability caused by LIX1L overexpression in NSCLC cells, indicating that NCL expression and rRNA synthesis participates in LIX1L-mediated biological functions during EMT. Collectively, our findings suggest that the LIX1L-NCL-rRNA synthesis axis is a novel EMT-activated mechanism. Targeting the pathway might be a therapeutic option for EMT and EGFR-TKIs resistance in NSCLC.

1. Introduction

Lung cancer is the leading cause of cancer-related death worldwide [1]. Non-small cell lung cancer (NSCLC) accounts for approximately 85% of lung cancer cases [2, 3]. For patients harboring specific epidermal growth factor receptor (EGFR) mutant genes, EGFR tyrosine kinase inhibitors (TKIs) are the first-line treatment with significant elimination of tumors [4, 5]. However, resistance to those drugs has been a serious challenge [6–8]. Several mechanisms are responsible for the resistance, such as alternative survival pathways bypassing the EGFR, secondary mutations in EGFR gene, transdifferentiation of NSCLC to the small cell lung cancer histotype, and formation of resistant tumors with mesenchymal characteristics in epithelial-mesenchymal transition (EMT) process [6, 7, 9–11].

EMT, an exemplar of cell plasticity in malignancies or development, can reversibly switch between epithelial and mesenchymal states in response to internal and external stimuli, with a regulatory network mainly consisting of transcription factors Snail1/2, Zeb1/2, and Twist1, which interacts with regulatory signals (TGF-β1, Notch-1, NF-κB, etc.) and downstream genes (such as CDH1, VIM, FN1) [12–14]. In cancer, the core functions of EMT, such as migration, invasion, outgrowth, escape from apoptosis, and therapy resistance, provide an advantage under various stress conditions [12, 14]. Therefore, identification of the EMT-activated mechanisms will provide therapeutic options for EMT and TKIs resistance in NSCLC.

Limb expression 1-like protein (LIX1L) might be an RNA binding protein involved in post-transcriptional regulation [15–18]. Recently, Byers et al. developed a robust 76-gene EMT signature that can predict resistance to EGFR and PI3K/Akt inhibitors [19], highlighting the different patterns of EGFR-TKI responses in epithelial and mesenchymal NSCLC cells. LIX1L was among the 76 genes and positively correlated with Vimentin and negatively correlated with E-cadherin [19]. A 37-gene EMT signature developed from

NCI-60 cell lines also showed that LIX1L might be a novel mesenchymal gene marker [20]. Functionally, LIX1L expression facilitated the migration and invasion of HCC cells [21]. Paradoxically, LIX1L knockdown enhanced migration and invasion in MDA-MB231 breast cancer cells [20]. These studies suggested that LIX1L might be a novel mesenchymal gene, but its biological function and mechanism in lung cancer EMT process remains unclear.

Ribosome biogenesis is a hallmark of cell proliferation. It occurs in nucleolus and is initiated by transcription of ribosomal DNA (rDNA) into rRNA by RNA polymerase I (POLR I) [22, 23]. The assembly of rRNA and ribosomal protein into mature ribosome underpins global protein synthesis in living organisms [24]. In tumor cells, the upregulation of ribosome biogenesis involves an alteration in the spectrum of translated mRNAs [23, 25]. Certain mRNAs, such as oncogenes, growth genes, and survival genes, have a low affinity for ribosome and are outcompeted by housekeeping gene mRNAs, when the number of ribosome is limited. On the contrary, an increase of ribosome biogenesis reduces this limiting factor and induces the translation of oncogene mRNAs to facilitate tumor progression. Most recently, it was reported that the hyperactivation of ribosome biogenesis is an important EMT feature and provides "fuel" for EMT program [26]. Snail1 could recruit to the rDNA repeats in a TGFβ1-dependent manner, inducing rRNA synthesis during EMT. POLR I inhibitor CX-5461 treatment blocked the association of Snail1 with rDNA to inhibit ribosome biogenesis, and specifically halted the gain of mesenchymal traits in NMuMG cells [26]. Single-cell RNA sequencing data from primary mouse tracheal epithelial cells indicated that ribosome biogenesis was significantly upregulated in hypoxia-induced EMT basal cells, and inhibition of ribosome biogenesis abrogated EMT in MTECs [27]. Collectively, these observations strongly suggest that EMT-associated ribosome biogenesis fuels EMT program and endows mesenchymal traits. Nevertheless, the roles of rRNA synthesis and the potential mechanisms in NSCLC EMT are unknown.

In this study, we demonstrate that the expression of LIX1L is positively correlated with mesenchymal markers in NSCLC tissues and is elevated in TGFβ1-induced EMT NSCLC cells. Interestingly, the increased LIX1L expression prominently localizes to the nucleoli and interacts with the key ribosome biogenesis regulator NCL protein, inducing rRNA synthesis in EMT NSCLC cells. LIX1L promotes cell migration, invasion, anoikis resistance, EGFR-TKIs resistance and proliferation at least in part by enhancing NCL expression and rRNA synthesis during EMT. Our study reveals that the LIX1L-NCL-rRNAsynthesis axis is a novel EMT-activated mechanism, and targeting the pathway might be a therapeutic option for EMT and EGFR-TKIs resistance in NSCLC.

2. Results

2.1. LIX1L expression is positively correlated with mesenchymal markers, lymphatic metastasis, and high TNM stage in NSCLC tumor specimens.

To investigate the correlation of LIX1L expression with EMT markers in clinical tumor specimens, we detected LIX1L, E-cadherin, and Vimentin expressions in 81 human NSCLC tissues by IHC assay. LIX1L expression was observed in the cytoplasm and nucleus of tumor cells (Fig. 1A). The positive rate of LIX1L

expression was 51.90% (42/81) and positively associated with lymphatic metastasis and high TNM stage (Table S1, $P < 0.0001$). E-cadherin expression was mainly located in the membrane of tumor cells (Fig. 1A) and the positive rate was 34.6% (28/81). E-cadherin expression is negatively associated with lymph node metastasis (Table S1, $P = 0.0361$) and TNM stage ($P = 0.0247$). Cytoplasm expression rate of Vimentin was 50.6% (41/81) and significantly correlated with lymph node metastasis (Fig. 1A, Table S1, $P = 0.001$). In addition, LIX1L expression was positively correlated with Vimentin expression (Fig. 1B; lung squamous cell carcinomas (LUAD), r = 0.483; lung adenocarcinomas (LUSC), r = 0.687; $P < 0.05$), while negatively correlated with E-cadherin expression (LUAD, r=-0.357; LUSC, r=-0.339; $P < 0.05$) in 41 LUAD and 40 LUSC specimens, respectively.

Next, we investigated the relationship between LIX1L and EMT markers at mRNA level in TCGA database. In 574 cases of LUAD, the correlation between LIXIL mRNA and CDH1 is low (Fig. 1C, r=-0.1037, $P = 0.0129$), while LIX1L is positively correlated with VIM (r = 0.4427, $P < 0.0001$) and ZEB1 (r = 0.5178, $P < 0.0001$). In 548 cases of LUSC, LIXIL expression is negatively correlated with CDH1 (Fig. 1C, r=-0.3245, $P < 0.0001$), and positively correlated with VIM (r = 0.6395, $P < 0.0001$) and ZEB1 (r = 0.5768, $P < 0.0001$). The above results indicated that LIX1L expression is positively correlated with mesenchymal markers at both mRNA and protein levels in NSCLC specimens.

2.2. LIX1L expression is significantly elevated in TGFβ1-treated EMT NSCLC cells.

Next, we treated H358, HCC827, and H1975 cells with TGFβ1 for 21d to induce EMT [28] and observed LIX1L expression in the cells. After TGFβ1 treatment, the cell morphology changed from cobblestone-like to elongated (Fig. 2A; Fig.S1A), accompanied by reduced E-cadherin expression and increased Vimentin expression (Fig. 2B, C; Fig.S1B, C). The results indicated that the TGFβ1-treated cells had undergone EMT (referred to as TGFβ1 cells thereafter). Compared with parental cells, the expression of LIX1L in TGFβ1 cells was significantly increased at both mRNA and protein levels (Fig. 2D, E; Fig.S1D, E). Besides, the microarray datasets (GSE49644) from GEO confirmed that LIX1L mRNA expression was increased in H358 (Log FC = 2.977, $P < 0.0001$) and HCC827 (Log FC = 2.852, $P < 0.0001$) cells treated with TGFβ1 for 48h (Fig. 2F). Taken together, the results from NSCLC tissues and cell lines indicated that LIX1L is a mesenchymal gene and might be functionally involved in the process of EMT.

2.3. Upregulated LIX1L expression promotes core EMT functions of NSCLC cells.

To investigate the biological functions of LIX1L during EMT, we knocked down LIX1L expression in H358-TGFβ1, HCC827-TGFβ1 (Fig. 3A), and H1975-TGFβ1 (Fig.S2A) cells using specific siRNA transfection *in vitro*. Transwells assay indicated that migration and invasion abilities were significantly decreased after LIX1L knockdown (Fig. 3B; Fig.S2B). CCK8 and clone formation assays showed that LIX1L knockdown significantly reduced cell proliferation (Fig. 3C, D; Fig.S2C, D). Resistance to anoikis is an important

characteristic of EMT and a critical contributor to tumor invasion and metastasis [29, 30]. Next, we induced cell anoikis by culturing the cells in Poly-HEMA coated plates [31, 32] and detected the apoptosis using Western blot and flow cytometry (FCM). Western blot showed that the active caspase-3 protein level in LIX1L knockdown cells was increased compared with control cells (Fig. 3E; Fig.S2E). FCM (PE Annexin V-7AAD apoptotic assay) indicated that the apoptotic (anoikis) rate was significantly increased after LIX1L knockdown in TGFβ1 cells (Fig. 3F; Fig.S2F). In addition, Western blot showed that E-cadherin expression was obviously induced, while Vimentin and Twist1 protein expressions were inhibited upon LIX1L knockdown (Fig. 3G; Fig.S2G). On the contrary, LIX1L overexpression in H358, HCC827, and H1975 cells (Fig. 3H; Fig.S2H) increased migration, invasion (Fig. 3I; Fig.S2I), proliferation (Fig. 3J; Fig.S2J), colony formation (Fig. 3K; Fig.S2K), and anoikis resistance (Fig. 3L; Fig.S2L) abilities. Besides, LIX1L overexpression inhibited E-cadherin protein expression and increased Vimentin and Twist1 protein expressions (Fig. 3M; Fig.S2M). Together, gain or loss of function assays indicated that LIX1L expression plays important functions in the EMT process of NSCLC cells.

2.4. LIX1L is localized in the nucleoli and impacts ribosomal RNA (rRNA) synthesis in TGFβ1-treated EMT NSCLC cells

In NSCLC specimens, we have detected that positive LIX1L expression is distributed in the cytoplasm and nucleus of tumor cells. Next, we determined the localization of LIX1L in EMT NSCLC cells using confocal immunofluorescent (IF). Interestingly, we found that LIX1L protein is enriched in the nucleus, especially in the nucleoli of TGFβ1 cells (Fig. 4A; Fig.S3A) compared with parental cells. Considering that rRNA synthesis and ribosome biogenesis occurs in nucleoli, we set out to investigate whether ribosome biogenesis was influenced by LIX1L expression during EMT. RT-qPCR results showed that 47s and 45s pre-rRNA (indicators of rRNA synthesis [33–35]) levels were significantly increased in TGFβ1 cells (Fig. 4B, C; Fig.S3B, C) compared with parental cells. Besides, H&E staining showed that the nucleolar size was increased (reflecting upregulation of ribosome biogenesis [25]) in TGFβ1 cells (Fig. 4D; Fig.S3D). LIX1L knockdown led to a significant decrease in 47s and 45s pre-rRNA expressions and nucleolus size (Fig. 4E-G; Fig.S3E-G). In contrast, overexpression of LIX1L significantly induced 47s and 45s pre-rRNA expressions in H358, HCC827 (Fig. 4H, I), and H1975 cells (Fig.S3H, I).

Next, we explored the effect of LIX1L on the expression of several key ribosome biogenesis regulators [33–35], including POLR I, nucleophosmin 1 (NPM1), fibrillarin (FBL), and nucleolin (NCL), during EMT. RT-qPCR showed that POLR I, NPM1, and FBL mRNA was increased significantly in TGFβ1 cells (Fig. 4J-L; Fig.S3J-L). NCL mRNA expression did not change obviously, but its protein expression was elevated in TGFβ1 cells (Fig. 4M, N; Fig.S3M, N). After LIX1L knockdown, only NCL mRNA was decreased in the three TGFβ1 cells (Fig. 4O-R, Fig.S3O-R). The above results indicated that the LIX1L expression plays a role in rRNA synthesis during EMT.

2.5. LIX1L interacts with NCL protein to regulate rRNA synthesis during EMT in NSCLC cells.

Similar to LIX1L, NCL is mainly located in nucleolus and regulates rRNA synthesis [33–35]. Next, we investigated the correlation between LIX1L and NCL expression in NSCLC cells. IF indicated that LIX1L and NCL protein were co-located in the nucleoli of TGFβ1 cells (Fig. 5A; Fig.S4A). Co-IP results confirmed the physical association between the endogenous LIX1L and NCL proteins (Fig. 5B; Fig.S4B) as well as between the exogenously expressed Flag-LIX1L and the endogenous NCL (Fig. 5C; Fig.S4C). Besides, LIX1L-NCL interaction was demonstrated in the nuclear extract of TGFβ1 cells (Fig. 5D; Fig.S4D). Next, we investigate the effect of LIX1L on NCL expression. Western blot showed that the NCL expression was obviously increased after LIX1L overexpression (Fig. 5E; Fig.S4E), but inhibited upon LIX1L knockdown (Fig. 5F; Fig.S4F). Besides, we performed LIX1L knockdown combined with MG132 (proteasome inhibitor) treatment and found that MG132 restored the reduced LIX1L and NCL protein levels due to LIX1L knockdown, suggesting that LIX1L and NCL protein might be degraded through proteasome pathway (Fig. 5G; Fig.S4G). NCL is critical for rRNA synthesis [36, 37]. We then knocked down NCL expression and observed a significant decrease in the 47s pre-rRNA level (Fig. 5H; Fig.S4H) and the size of nucleoli (Fig. 5I; Fig.S4I) in TGFβ1 cells. Furthermore, we investigated the role of NCL in LIX1L-induced rRNA synthesis during EMT. RT-qPCR showed that NCL knockdown partially reversed the enhanced rRNA synthesis due to LIX1L overexpression (Fig. 5J; Fig.S4J). These results indicated that LIX1L physically interacts with NCL and promotes its expression in EMT NSCLC cells, which might be the mechanism of LIX1L involved in the rRNA synthesis during EMT.

2.6. LIX1L-NCL promotes proliferation and core EMT functions of NSCLC cells.

To investigate the biological functions of NCL during EMT, we knocked down its expression in H358-TGFβ1, HCC827-TGFβ1, and H1975-TGFβ1 cells using specific siRNA transfection (Fig. 6A; Fig.S5A). NCL Knockdown resulted in a significant decrease in migration and invasion (Fig. 6B; Fig.S5B, $P < 0.05$), cell proliferation (Fig. 6C; Fig.S5C, $P < 0.05$), colony formation (Fig. 6D; Fig.S5D, $P < 0.05$), and anoikis resistance (Fig. 6E, F; Fig.S5E, F, $P < 0.05$), accompanied with upregulated E-cadherin expression and reduced Vimentin and Twist1 expressions (Fig. 6G; Fig.S5G). These results indicated that NCL plays important functions in the EMT process of NSCLC cells.

To elucidate whether NCL participates in LIX1L-mediated core EMT functions, we knocked down NCL expression in LIX1L overexpression cells. Transwells results showed that NCL knockdown reversed the increased migration and invasion abilities due to LIX1L overexpression (Fig. 6H; Fig.S5H, $P < 0.05$). CCK8 and clone formation assays showed that NCL knockdown abrogated LIX1L overexpression-induced proliferation (Fig. 6I, J; Fig.S5I, J, $P < 0.05$). The above results indicated that NCL plays a role in LIX1L-mediated EMT functions of NSCLC cells.

2.7. NCL protein is correlated with LIX1L expression, mesenchymal markers, lymphatic metastasis, and high TNM stage in NSCLC tumor specimens.

Next, we evaluate NCL expression in the 81 NSCLCs using IHC. NCL staining was mainly detected in the nucleus of tumor cells (Fig.S6A, B). Positive expression rate of NCL was 70.4% (57/81) and positively correlated with lymphatic metastasis and high TNM stage (Table S2, $P < 0.0001$). Besides, a positive correlation was observed between NCL and LIX1L (Fig.S6C, D; LUAD, r = 0.417, $P = 0.024$; LUSC, r = 0.526, $P < 0.01$), as well as between NCL and Vimentin (Fig.S6C, D; LUAD, r = 0.358, $P = 0.012$; LUSC, r = 0.437, $P = 0.0338$) in 41 LUAD and 40 LUSC specimens, respectively.

2.8. Inhibition of rRNA synthesis by CX-5461 inhibits cell proliferation and core EMT functions of NSCLC cells

To examine the effect of rRNA synthesis on EMT process of NSCLC cells, we employed CX-5461 to inhibit rRNA synthesis [26]. CX-5461 treatment in TGFβ1 cells led to a significant reduction in 47s pre-rRNA expression (Fig. 7A; Fig.S7A, $P < 0.05$), accompanied by decreased migration, invasion (Fig. 7B; Fig.S7B, $P < 0.05$), proliferation (Fig. 7C, D; Fig.S7C, D, $P < 0.05$), and anoikis resistance (Fig. 7E, F; Fig.S7E, F, $P < 0.05$). In addition, CX-5461 also significantly reduced the expression of Vimentin and Twist1 protein (Fig. 7G; Fig.S7G).

Next, we performed LIX1L overexpression combined with CX-5461 treatment in H358, HCC827, and H1975 cells to elucidate whether rRNA synthesis participated in LIX1L-mediated biological functions. Transwells assay demonstrated that CX-5461 significantly reversed the enhanced migration and invasion due to LIX1L overexpression (Fig. 7H; Fig.S7H, $P < 0.05$). CCK8 and clone formation assays showed that CX-5461 treatment partially abrogated the LIX1L overexpression-induced proliferation (Fig. 7I, J; Fig.S7I, J, $P < 0.05$). These results suggested that rRNA synthesis is required for LIX1L to execute EMT in NSCLC cells.

2.9. Upregulated LIX1L enhances EGFR-TKIs resistance in TGFβ1-treated EMT NSCLC cells in part by upregulating NCL expression and rRNA synthesis.

To investigate the effects of LIXIL on EGFR-TKIs resistance, cell response to gefitinib or erlotinib treatment was detected using CCK8 method. Compared to parental cells, the viabilities of H358-TGFβ1, HCC827-TGFβ1, and H1975-TGFβ1 cells were all significantly increased upon gefitinib (Fig. 8A; Fig.S8A, $P < 0.05$) or erlotinib (Fig. 8B; Fig.S8B, $P < 0.05$) treatment. IC_{50} value indicated that TGFβ1 cells were more resistant to gefitinib and erlotinib compared to parental cells (Fig. 8C; Fig.S8C, $P < 0.05$). LIX1L knockdown in TGFβ1 cells decreased the cell resistance to gefitinib and erlotinib treatment, and the IC_{50} value is decreased correspondingly (Fig. 8D-F; Fig.S8D-F, $P < 0.05$). In contrast, overexpression of LIX1L significantly promoted cell resistance to gefitinib and erlotinib in H358, HCC827, and H1975 cells (Fig. 8G-I; Fig.S8G-I, $P < 0.05$). These results indicated that LIX1L expression is positively correlated with EGFR-TKIs resistance in NSCLC cells.

Next, we explore whether NCL expression and rRNA synthesis participate in the LIX1L-mediated EGFR-TKIs resistance. As shown in Fig. 8J-M and Fig.S8J-M, overexpression of LIX1L significantly promoted cell resistance to gefitinib and erlotinib, which is consistent with the above results in Fig. 8G-I and

Fig.S8G-I. However, silencing NCL (Fig. 8J, K; Fig.S8J, K, $P < 0.05$) or treating with CX-5461 (Fig. 8L, M; Fig.S8L, M, $P < 0.05$) significantly reversed LIX1L-induced cell resistance to gefitinib and erlotinib treatment. Together, the above data suggested that LIX1L expression enhances EGFR-TKIs resistance in TGFβ1-treated EMT NSCLC cells in part through upregulated NCL expression and rRNA synthesis.

3. Discussion

Nucleoli are the subdomains of nucleus that form around actively transcribed rRNA genes. They serve as the site of rRNA synthesis and processing, and ribosome assembly [22, 23]. Pol I transcribes rDNA to produce 47S pre-rRNA within nucleoli [38]. Therefore, nucleolar size reflects the functional activity of rRNA synthesis and ribosome biogenesis [25]. Besides, NCL protein, a key ribosome biogenesis regulator, also mainly distributes in nucleoli [39, 40]. Here, we demonstrate that the protein of LIX1L prominently translocates to the nucleoli of NSCLC cells during EMT, where it induces rRNA synthesis, through physical association with NCL protein, accompanied by increased nucleolar size. Hyperactivation of rRNA synthesis and ribosome biogenesis leads to not only an increases in global protein synthesis [24], but also an alteration in the spectrum of translated mRNAs from housekeeping genes to oncogenes, growth genes, and survival genes expression [23, 25], triggering tumor progression. Consistent with these reports, we demonstrate that LIX1L promotes cell migration, invasion, proliferation, anoikis resistance, and EGFR-TKIs resistance through NCL-mediated rRNA synthesis in EMT NSCLC cells (Fig. 9N).

LIX1L is first identified as a key regulator of proliferation in acute myeloblastic leukemia cells [41]. Subsequent data revealed that LIX1L is overexpressed in human HCC and has an oncogenetic role mainly through miRNAs (such as miR-21-3p, miR-6089, and miR-1269) regulation [21, 42, 43]. Although Nakamura et al. detected the expression of LIX1L protein in several types of cancers, the clinical significance of LIX1L is unavailable [15]. In this study, IHC analysis in 81 NSCLC specimens showed that LIX1L expression is positively associated with lymphatic metastasis, high TNM stage and Vimentin expression, but is negatively correlated with E-cadherin expression. TCGA data indicated that LIXIL mRNA expression is positively correlated with mesenchymal markers Vimentin and ZEB1. Besides, LIX1L expression is significantly elevated in TGFβ1-induced EMT NSCLC cells and promotes EMT process. Together, our results reveal that LIX1L is a novel mesenchymal gene and involved in the EMT-associated biological function in NSCLC.

NCL is an RNA-binding protein that participates in DNA transcription, ribosomal biogenesis, and post-transcriptional regulation [39, 40, 44, 45]. It physically associates with miRNAs, lncRNAs, as well as mRNAs and regulates the modification and metabolism of these molecules to control specific gene expression [46, 47]. The level of NCL is increased in highly proliferating cells, and higher NCL expression correlates with more growth and metastasis of tumors [46, 48, 49]. In lung cancer, NCL expression is induced by EGFR signaling and correlates with poor prognosis [50]. Consistent with these reports, our IHC data from 81 NSCLCs showed that NCL expression is positively correlated with lymphatic metastasis, high TNM stage, LIX1L expression, and Vimentin expression. Recent studies indicated that NCL expression is involved in EMT process. For example, NCL could directly interact with the lncRNA CYTOR

to form a complex, which activates EMT and NF-κB pathways to promote CRC progression [51]. CPNE7 mediates signal transduction and metastasis in many tumors. NCL could bind with CPNE7 to activate NF-κB pathway, promoting cancer metastasis through EMT in mesenchymal stromal cells derived from oral squamous cell carcinoma [52]. The present study indicates that NCL protein expression is induced in TGFβ1-treated EMT cells and plays important functions in EMT process. Knockdown of NCL decreases migration, invasion, proliferation, anoikis resistance, and EGFR-TKIs resistance, accompanied by upregulated E-cadherin and downregulated Vimentin and Twist1 protein expression. Besides, NCL participates in LIX1L mediated rRNA synthesis and EMT-related function, such as migration, invasion, proliferation, and EGFR-TKIs resistance in EMT NSCLC cells.

Ribosome biogenesis is emerging as a necessary feature of EMT program. Inhibition of the initiation of ribosome biogenesis by CX-5461 halts mesenchymal gene expression and induces the differentiation from a basal-like to a luminal ERα + phenotype in mammary cancer cells [26]. Inhibition of rRNA synthesis resulted in mesenchymal-epithelial transformation during mouse implantation and decidualization *in vitro* [53]. Using the Mx1-Cre system to specifically knock out Zeb1 in adult hematopoietic stem cells, ribosome biogenesis was downregulated in Zeb1−/−EpCAM + HSPCs [54]. In addition, treacle ribosome biogenesis factor 1 regulates KRAS-activated genes and EMT genes in HCC and is required for the increased rRNA production [55]. Consistent with the above reports, we show that rRNA synthesis is elevated in EMT NSCLC cells and inhibition of rRNA synthesis suppresses cell migration, invasion, proliferation, anoikis resistance, and EGFR-TKIs resistance, accompanied by downregulated Vimentin and Twist1 protein expression. Besides, rRNA synthesis participates in LIX1L mediated cell proliferation, migration, invasion, and EGFR-TKIs resistance in TGFβ1-induced EMT NSCLC cells. Furthermore, our results demonstrate that LIX1L induces rRNA synthesis at least in part by enhancing NCL protein expression during EMT. Collectively, we reveal that the LIX1L-NCL-rRNA synthesis axis is critical for the EMT process induced by TGFβ1 in NSCLC cells.

In summary, this study demonstrates that LIX1L is a novel mesenchymal gene and functionally involved in the process of EMT via NCL-mediated ribosomal RNA synthesis in NSCLC. Blocking NCL expression and rRNA synthesis may provide a useful new strategy for lung cancer therapy.

4. Materials And Methods

4.1. Patients and clinical specimens

The present study protocol was approved by the Institutional Review Committee of Hebei Medical University. All patients consented to the study. We randomly selected and reviewed the medical records of 81 patients with primary NSCLC in the Second Hospital of Hebei Medical University from 2010 to 2013. The formalin-fixed paraffin-embedded (FFPE) surgical tumor specimens were cut into 4μm sections and the clinicopathological feature data were summarized for further investigation.

4.2. Cell culture and treatment

NCI-H358, HCC827, and H1975 human NSCLC cell lines were obtained from Beijing Cell Resource Center (Institute of Basic Medicine, Chinese Academy of Medical Sciences) and authenticated by STR profiling. Cells were cultured in basal medium (Gibco) supplemented with 10% fetal bovine serum (Gemini), 100 units/ml penicillin, and 0.1mg/ml streptomycin (BI). Cells were cultured at 37°C in 5% CO_2 incubator and were routinely detected for mycoplasma. Cells were treated with recombinant human TGF-β1 (Gibco) 5ng/ml for 21d to construct EMT models [28]. To inhibit rRNA synthesis, CX-5461 (100 nM) was employed for 24 h for subsequent detection [26]. MG132 (20μM) was added to the medium and maintained for 6h to block the proteasome-dependent degradation pathway.

4.3. RNA interference and gene overexpression (RNAi and OE)

Cells were transiently transfected with small interfering RNAs (siRNAs) to inhibit gene expression. The siRNAs were synthesized by GenePharma (Shanghai, China), with sequences as follows:

siRNA-Lix1l sense, 5'-GGAGGAGUGCUGCAAAGAUTT-3';

siRNA-Lix1l reverse, 5'-AUGUUUGCAGCACUCCUCCTT-3';

siRNA-NCL sense, 5'-AAGAGCCUGUCAAAGAAUUTT-3';

siRNA-NCL reverse, 5'-AAUUCUUUGACAGGCUCUUCC-3';

siRNA-negative control (NC) sense, 5'-UUCUCCGAACGUGUCACGUTT-3';

siRNA-NC reverse, 5'-ACGUGACACGUUCGGAGAATT-3'.

The LIX1L-Flag plasmidwas constructed in pEZ-Lv203 vector (GeneCopoeia). Lipofectamine^{2000}(Invitrogen) was used for cell transfection in accordance with the manufacturer's protocol.

4.4. RNA isolation, complementary DNA synthesis, and quantitative real time PCR (RT-qPCR)

Total cell RNA was isolated using TRIzol reagent (Invitrogen). The mRNA complementary DNA was synthesized using GoScript Reverse Transcription System (Promega), followed by polymerase chain reaction (Agilent Mx3000/5P) amplification with PCR Mix (Promega) in accordance with the manufacturer's instructions. β-actin was used as an internal control. Expression of each target was calculated using the 2-ΔΔCt method, which presented relative expression. The mRNA primer sequences are listed in supplementary information Table S1.

4.5. Western blot analysis (WB)

Cells were lysed at 4°C in lysis buffer supplemented with Protease Inhibitor Cocktail (APExBIO). Total cellular protein concentration was measured with the BCA kit (Pierce) and 15 μg protein per lane was

separated in SDS-PAGE and transferred to PVDF membranes (Bio-Rad). Blots were blocked with 5% skimmed milk powder in TBS with 0.1% Tween 20 for 60 min at 37°C, and incubated with specific antibodies at 4°C overnight. The blots were probed with HRP-conjugated affinipure secondary antibodies (Proteintech, IL, USA), visualized by the chemiluminescence, and scanned using ImageQuant LAS 4010 Imaging System (GE Healthcare Life Sciences, Piscataway, NJ). Equal loading of protein was confirmed by reprobing membranes for β-actin as a loading control. The specific antibodies are listed in supplementary information Fig.S2.

4.6. Nuclear extract preparation and co-immunoprecipitation (Co-IP)

Extraction of nuclear proteins was conducted using Minute Cytoplasmic and Nuclear Extraction Kit (sc-003, Invent) according to the manufacturer's instructions. Briefly, 500μl cytoplasmic extraction buffer containing 5μl Protease Inhibitor Cocktail (APExBIO) was added to the cell flash on ice for 5 min and the lysed cells were centrifuged. The pellet was washed and then nuclear extraction buffer was added to the pellet. After incubation on ice and filtration, the nuclear extract was collected.

Co-IP assay was performed using Protein A/G PLUS-Agarose (sc-2003, SANTA CRUZ) in accordance with the manufacturer's instructions. Briefly, whole cell lysate and nuclear extract were supplemented with Protease Inhibitor Cocktail and precleared by adding IgG and Protein A/G PLUS-Agarose, followed by incubation at 4°C for 30 min. After centrifugation, the supernatant was added with primary antibody and IgG (1μg) and incubated at 4°C for 120 min, respectively. Subsequently, 50 μl Protein A/G PLUS-Agarose was added and incubation was conducted on a rocker platform at 4°C overnight. Next, immunoprecipitates were washed with PBS 4 times, and 40 μl electrophoresis sample buffer was added to the immunoprecipitates, followed by boiling samples for 5 min and detection of WB. The antibodies were presented in supplementary information Fig.S2.

4.7. Morphological observation and Laser confocal immunofluorescence detection (IF)

When cultured to 70% confluence in the 6-well plate, cells were fixed in 4% neutral paraformaldehyde for 30 min and observed under phase contrast microscopy. For IF study, cells were seeded in a 24-well plate with a sterile glass slide at the bottom, cultured for 24 h, and fixed in paraformaldehyde for 30 min. After washing with PBS, the cells were incubated in 4% Bovine Serum Albumin and 0.5% tritonX 100 for 60 min at 37°C, and then incubated in primary antibodies at 4°C overnight. After washing with PBS for 15 min, cells were incubated in Fluorescein (FITC)-conjugated Affinipure Goat Anti-Rabbit IgG (H + L) and Fluorescein (Cy3)-conjugated Affinipure Goat Anti-Mouse IgG (H + L) diluted at 1:200 for 60 min at 37°C in dark. Cells were counterstained with DAPI (Sigma) and observed using a laser confocal microscope (Leica TCS SP8).

4.8. Haematoxylin and eosin (H&E)-staining and nucleolar size evaluation

The cell-climbing sheets were fixed with methanol for 30 min. After washing with distilled water for 10min, the sheets were stained with hematoxylin and eosin, respectively. Then the sheets were dehydrated with alcohol, soaked in xylene and sealed with neutral gum. The nucleoli were stained purple by H&E-staining method and nucleolar size was graded according to the following algorithm: 1) Lack of nucleoli or nucleoli present but inconspicuous (size low); 2) prominent nucleoli or macronucleoli (size high).

4.9. Immunohistochemistry (IHC)

The IHC assay was performed using SP-9001 IHC kit (ZSGB-BIO, Beijing, China). H_2O_2 (5%) was employed to eliminate endogenous peroxidase activity. After incubation in 5% normal goat serum for 30 min to block non-specific binding, the sections were incubated with primary antibody at 4°C overnight followed by a biotinylated goat secondary antibody at 37°C for 45 min. Next, the sections were treated with streptavidin labeled with horseradish peroxidase for 60 min at 37°C and were stained with diaminobenzidine (DAB) and counterstained with hematoxylin. The sections were observed under the microscope (Olympus, Japan) and photographs were acquired (400×) using LAS V4.9 (Leica, Germany). Stained cells were counted and the positive staining rate was analyzed in five random fields for each sample. The primary antibodies were presented in Supporting Information Fig.S2.

4.10. Cell proliferation and colony formation assays

Cells were seeded into 96-well plates (1000 cells per well) in the standard culture condition. After 24, 48, 72, and 96 h, each well was added with Cell Counting Kit-8 reagent (CCK-8, Dojindo, China) for 2 h, and the proliferation of cells was assessed by measuring the absorbance of optical density (OD) at 450 nm wavelength in five replicates. For colony formation assay, the cells were seeded into 6-well plates with 500 cells per well and cultured for 10–14 d in normal medium replaced twice a week. After 10–14 d, the colonies were fixed with 4% neutral paraformaldehyde for 30 min, stained with 0.1% crystal violet for 30 min, and then counted and taken pictures.

4.11. Migration and invasion assays

Transwell chambers (8μm pore, BD Biosciences) were utilized for migration and invasion studies. The transwell chambers with (for invasion assay) or without (for migration assay) Matrigel (BD Biosciences) were placed in 24-well plates, and the suspension with 4×10^4 cells was added to the chamber, followed by adding 500 μL medium supplemented with 10% FBS to the 24-well plates. After incubation for 24-48h, the cells on the lower surface of the chambers were fixed with 4% formalin for 30min, stained with crystal violet for 30min, counted and photographed using a light microscope (Olympus, Japan).

4.12. Drug sensitivity assay and 50% inhibitory concentration (IC_{50}) detection

Cells were seeded into 96-well plates with 2.5×10^4 cells/well, cultured for 24 h, and added with different concentrations (0.005-80μM) of gefitinib/erlotinib, respectively. After 48 h, CCK-8 was added to each well (10 μl/well) for 2 h. The absorbance (A) at 450 nm was measured using a microplate reader (ELx800,

BioTek), and the cell survival rate was calculated using the following formula: cell survival rate = (Treatment group A – non-cellular group A) / (NC group A – non-cellular group A). The 50% inhibitory concentration (IC_{50}) was calculated according to the relative survival curve using GraphPad Prism 6 (GraphPad Software).

4.13. Anoikis assay

To induce anoikis [31, 32], trypsinized cells were seeded into 6-well plates (3×10^5/well) that had been coated with Poly (2-hydroxyethyl methacrylate) (poly-HEMA, #SLCF8468, SIGMA). The cells were then cultured for 18–24 h for further study. Poly-HEMA plates were made by applying 1.5 ml of a 10 mg/ml solution of poly-HEMA in alcohol into the well, drying in a cell incubator at 37°C for 12h, followed by washing with PBS.

4.14. Apoptosis detection

To quantify the cells of apoptosis, PE Annexin V-7AAD Apoptosis Detection Kit (BD Biosciences) was employed to stain cells in accordance with the manufacturer's protocols, and the cells were detected with FACScan flow cytometer (BD Biosciences). The data were analyzed with FlowJo software. In addition, the apoptosis was also assessed by Western Blot with active caspase 3 (apoptosis implementing protein) antibody.

4.15. Statistical analysis

Statistical Product and Service Solutions (SPSS) 13.0 (Chicago, IL, USA) and GraphPad Prism 6 (La Jolla, CA, USA) software were used for statistical analysis. The data in this study met the assumption of normal distribution and were shown as the mean ± standard deviation (SD). The differences between groups were assessed by using Students'-test or χ^2-test method and correlations were tested by Spearman correlation or Person correlation analysis. All experiments were performed at least 3 replicates. Results were considered statistically significant at p value less than 0.05.

Declarations

ACKNOWLEDGMENT

We thank the staff of the pathology department of the second hospital of Hebei Medical University for completing IHC assay.

CONFLICT OF INTERESTS

The authors declare that they have no competing interests.

AUTHOR CONTRIBUTIONS

LX performed study concept and design, and wrote the paper. ML contributed to IHC, *in vitro* analyses, and writing. JZ, XM and BL helped to perform cell culture and treatment. SM X participated in writing and revising the manuscript. FL, DY, and JGZ helped to perform in IHC and data analysis. HS help to perform the FCM analysis. All authors have read and approved the final manuscript.

ETHICS

The study was approved and reviewed by the Institutional Review Committee of Hebei Medical University (Shijiazhuang, Hebei, China). All patients have consented to the study.

FUNDING

This work was supported by Grants 81572275 from the National Natural Science Foundation of China, Grants U20A20369 from the National Natural Science Foundation of China, Grants H2020206234 from Natural Science Foundation of Hebei province, China, and Grants WZYCZY202003 from Bureau of Science and Technology of Hebei Province, China.

DATA AVAILABILITY

The authors declare that the data supporting the findings of this study are available within the article and Supplementary Information.

References

1. Sung H, Ferlay J, Siegel RL, Laversanne M, Soerjomataram I, Jemal A, et al. Global Cancer Statistics 2020: GLOBOCAN Estimates of Incidence and Mortality Worldwide for 36 Cancers in 185 Countries. CA Cancer J Clin. 2021;71:209–249.
2. Chen Z, Fillmore CM, Hammerman PS, Kim CF, Wong KK. Non-small-cell lung cancers: a heterogeneous set of diseases. Nat Rev Cancer. 2014;14:535–546.
3. Miller KD, Nogueira L, Mariotto AB, Rowland JH, Yabroff KR, Alfano CM, et al. Cancer treatment and survivorship statistics, 2019. CA Cancer J Clin. 2019;69:363–385.
4. Ettinger DS, Wood DE, Aisner DL, Akerley W, Bauman JR, Bharat A, et al. NCCN Guidelines Insights: Non-Small Cell Lung Cancer, Version 2.2021. J Natl Compr Canc Netw. 2021;19:254–266.
5. Kancha RK, von Bubnoff N, Peschel C, Duyster J. Functional analysis of epidermal growth factor receptor (EGFR) mutations and potential implications for EGFR targeted therapy. Clin Cancer Res. 2009;15:460–467.
6. Tulchinsky E, Demidov O, Kriajevska M, Barlev NA, Imyanitov E. EMT: A mechanism for escape from EGFR-targeted therapy in lung cancer. Biochim Biophys Acta Rev Cancer. 2019;1871:29–39.
7. Zhu X, Chen L, Liu L, Niu X. EMT-Mediated Acquired EGFR-TKI Resistance in NSCLC: Mechanisms and Strategies. Front Oncol. 2019;9:1044.

8. Ohashi K, Maruvka YE, Michor F, Pao W. Epidermal growth factor receptor tyrosine kinase inhibitor-resistant disease. J Clin Oncol. 2013;31:1070–1080.
9. Zhang Z, Lee JC, Lin L, Olivas V, Au V, LaFramboise T, et al. Activation of the AXL kinase causes resistance to EGFR-targeted therapy in lung cancer. Nat Genet. 2012;44:852–860.
10. Ji W, Choi YJ, Kang MH, Sung KJ, Kim DH, Jung S, et al. Efficacy of the CDK7 Inhibitor on EMT-Associated Resistance to 3rd Generation EGFR-TKIs in Non-Small Cell Lung Cancer Cell Lines. Cells. 2020;9.
11. Pan G, Liu Y, Shang L, Zhou F, Yang S. EMT-associated microRNAs and their roles in cancer stemness and drug resistance. Cancer Commun (Lond). 2021;41:199–217.
12. Brabletz S, Schuhwerk H, Brabletz T, Stemmler MP. Dynamic EMT: a multi-tool for tumor progression. EMBO J. 2021;40:e108647.
13. Erin N, Grahovac J, Brozovic A, Efferth T. Tumor microenvironment and epithelial mesenchymal transition as targets to overcome tumor multidrug resistance. Drug Resist Updat. 2020;53:100715.
14. Yang J, Antin P, Berx G, Blanpain C, Brabletz T, Bronner M, et al. Guidelines and definitions for research on epithelial-mesenchymal transition. Nat Rev Mol Cell Biol. 2020;21:341–352.
15. Nakamura S, Kahyo T, Tao H, Shibata K, Kurabe N, Yamada H, et al. Novel roles for LIX1L in promoting cancer cell proliferation through ROS1-mediated LIX1L phosphorylation. Sci Rep. 2015;5:13474.
16. Zhu X, Zhang Y, Zhao Y, Xiang D, Zou J, Andrisani O, et al. LIX1-like protein drives hepatic stellate cell activation to promote liver fibrosis by regulation of chemokine mRNA stability. Signal Transduct Target Ther. 2021;6:319.
17. Pereira B, Billaud M, Almeida R. RNA-Binding Proteins in Cancer: Old Players and New Actors. Trends Cancer. 2017;3:506–528.
18. Robichaud N, del Rincon SV, Huor B, Alain T, Petruccelli LA, Hearnden J, et al. Phosphorylation of eIF4E promotes EMT and metastasis via translational control of SNAIL and MMP-3. Oncogene. 2015;34:2032–2042.
19. Byers LA, Diao L, Wang J, Saintigny P, Girard L, Peyton M, et al. An epithelial-mesenchymal transition gene signature predicts resistance to EGFR and PI3K inhibitors and identifies Axl as a therapeutic target for overcoming EGFR inhibitor resistance. Clin Cancer Res. 2013;19:279–290.
20. Rajapakse VN, Luna A, Yamade M, Loman L, Varma S, Sunshine M, et al. CellMinerCDB for Integrative Cross-Database Genomics and Pharmacogenomics Analyses of Cancer Cell Lines. iScience. 2018;10:247–264.
21. Zou J, Zhu X, Xiang D, Zhang Y, Li J, Su Z, et al. LIX1-like protein promotes liver cancer progression via miR-21-3p-mediated inhibition of fructose-1,6-bisphosphatase. Acta Pharm Sin B. 2021;11:1578–1591.
22. Orsolic I, Jurada D, Pullen N, Oren M, Eliopoulos AG, Volarevic S. The relationship between the nucleolus and cancer: Current evidence and emerging paradigms. Semin Cancer Biol. 2016;37–38:36–50.

23. Pelletier J, Thomas G, Volarevic S. Ribosome biogenesis in cancer: new players and therapeutic avenues. Nat Rev Cancer. 2018;18:51–63.
24. Bohnsack KE, Bohnsack MT. Uncovering the assembly pathway of human ribosomes and its emerging links to disease. EMBO J. 2019;38:e100278.
25. Quin JE, Devlin JR, Cameron D, Hannan KM, Pearson RB, Hannan RD. Targeting the nucleolus for cancer intervention. Biochim Biophys Acta. 2014;1842:802–816.
26. Prakash V, Carson BB, Feenstra JM, Dass RA, Sekyrova P, Hoshino A, et al. Ribosome biogenesis during cell cycle arrest fuels EMT in development and disease. Nat Commun. 2019;10:2110.
27. Hou Y, Ding Y, Du D, Yu T, Zhou W, Cui Y, et al. Airway Basal Cells Mediate Hypoxia-Induced EMT by Increasing Ribosome Biogenesis. Front Pharmacol. 2021;12:783946.
28. Yuan JH, Yang F, Wang F, Ma JZ, Guo YJ, Tao QF, et al. A long noncoding RNA activated by TGF-beta promotes the invasion-metastasis cascade in hepatocellular carcinoma. Cancer Cell. 2014;25:666–681.
29. Cao Z, Livas T, Kyprianou N. Anoikis and EMT: Lethal "Liaisons" during Cancer Progression. Crit Rev Oncog. 2016;21:155–168.
30. Redfern AD, Spalding LJ, Thompson EW. The Kraken Wakes: induced EMT as a driver of tumour aggression and poor outcome. Clin Exp Metastasis. 2018;35:285–308.
31. Frisch SM, Francis H. Disruption of epithelial cell-matrix interactions induces apoptosis. J Cell Biol. 1994;124:619–626.
32. Meredith JE, Jr., Fazeli B, Schwartz MA. The extracellular matrix as a cell survival factor. Mol Biol Cell. 1993;4:953–961.
33. Brombin A, Joly JS, Jamen F. New tricks for an old dog: ribosome biogenesis contributes to stem cell homeostasis. Curr Opin Genet Dev. 2015;34:61–70.
34. Fournier E, Heiblig M, Lespinasse C, Flandrin-Gresta P, Geay A, Miguet L, et al. Molecular heterogeneity and measurable residual disease of rare NPM1 mutations in acute myeloid leukemia: a nationwide experience from the GBMHM study group. Leukemia. 2022.
35. Baltanas FC, Berciano MT, Tapia O, Narcis JO, Lafarga V, Diaz D, et al. Nucleolin reorganization and nucleolar stress in Purkinje cells of mutant PCD mice. Neurobiol Dis. 2019;127:312–322.
36. Rickards B, Flint SJ, Cole MD, LeRoy G. Nucleolin is required for RNA polymerase I transcription in vivo. Mol Cell Biol. 2007;27:937–948.
37. Jia W, Yao Z, Zhao J, Guan Q, Gao L. New perspectives of physiological and pathological functions of nucleolin (NCL). Life Sci. 2017;186:1–10.
38. Xuan J, Gitareja K, Brajanovski N, Sanij E. Harnessing the Nucleolar DNA Damage Response in Cancer Therapy. Genes (Basel). 2021;12.
39. Roger B, Moisand A, Amalric F, Bouvet P. Nucleolin provides a link between RNA polymerase I transcription and pre-ribosome assembly. Chromosoma. 2003;111:399–407.

40. Sengupta TK, Bandyopadhyay S, Fernandes DJ, Spicer EK. Identification of nucleolin as an AU-rich element binding protein involved in bcl-2 mRNA stabilization. J Biol Chem. 2004;279:10855–10863.
41. Nakamura S, Nagata Y, Tan L, Takemura T, Shibata K, Fujie M, et al. Transcriptional repression of Cdc25B by IER5 inhibits the proliferation of leukemic progenitor cells through NF-YB and p300 in acute myeloid leukemia. PLoS One. 2011;6:e28011.
42. Shen C, Xu Y, Lu TF, Zhang JJ, Qian YB, Xu N. LncRNA TATDN1 induces the progression of hepatocellular carcinoma via targeting miRNA-6089. Eur Rev Med Pharmacol Sci. 2019;23:6459–6466.
43. Gan T, Tang R, He R, Dang Y, Xie Y, Chen G. Upregulated MiR-1269 in hepatocellular carcinoma and its clinical significance. Int J Clin Exp Med. 2015;8:714–721.
44. Serin G, Joseph G, Faucher C, Ghisolfi L, Bouche G, Amalric F, et al. Localization of nucleolin binding sites on human and mouse pre-ribosomal RNA. Biochimie. 1996;78:530–538.
45. Abdelmohsen K, Tominaga K, Lee EK, Srikantan S, Kang MJ, Kim MM, et al. Enhanced translation by Nucleolin via G-rich elements in coding and non-coding regions of target mRNAs. Nucleic Acids Res. 2011;39:8513–8530.
46. Sheetz T, Mills J, Tessari A, Pawlikowski M, Braddom AE, Posid T, et al. NCL Inhibition Exerts Antineoplastic Effects against Prostate Cancer Cells by Modulating Oncogenic MicroRNAs. Cancers (Basel). 2020;12.
47. Luo H, Zhang Y, Deng Y, Li L, Sheng Z, Yu Y, et al. Nxhl Controls Angiogenesis by Targeting VE-PTP Through Interaction With Nucleolin. Front Cell Dev Biol. 2021;9:728821.
48. Romano S, Fonseca N, Simoes S, Goncalves J, Moreira JN. Nucleolin-based targeting strategies for cancer therapy: from targeted drug delivery to cytotoxic ligands. Drug Discov Today. 2019;24:1985–2001.
49. Carvalho LS, Goncalves N, Fonseca NA, Moreira JN. Cancer Stem Cells and Nucleolin as Drivers of Carcinogenesis. Pharmaceuticals (Basel). 2021;14.
50. Hsu TI, Lin SC, Lu PS, Chang WC, Hung CY, Yeh YM, et al. MMP7-mediated cleavage of nucleolin at Asp255 induces MMP9 expression to promote tumor malignancy. Oncogene. 2015;34:826–837.
51. Wang X, Yu H, Sun W, Kong J, Zhang L, Tang J, et al. The long non-coding RNA CYTOR drives colorectal cancer progression by interacting with NCL and Sam68. Mol Cancer. 2018;17:110.
52. Ji X, Sun T, Xie S, Qian H, Song L, Wang L, et al. Upregulation of CPNE7 in mesenchymal stromal cells promotes oral squamous cell carcinoma metastasis through the NF-kappaB pathway. Cell Death Discov. 2021;7:294.
53. Liang YX, Hu W, Jin ZY, Diao HL, Liu L, Yang Y, et al. Nucleolar stress regulates stromal-epithelial transition via NPM1 during decidualization. Reproduction. 2020;160:491–500.
54. Almotiri A, Alzahrani H, Menendez-Gonzalez JB, Abdelfattah A, Alotaibi B, Saleh L, et al. Zeb1 modulates hematopoietic stem cell fates required for suppressing acute myeloid leukemia. J Clin Invest. 2021;131.

55. Wu C, Xia D, Wang D, Wang S, Sun Z, Xu B, et al. TCOF1 coordinates oncogenic activation and rRNA production and promotes tumorigenesis in HCC. Cancer Sci. 2022;113:553–564.

Figures

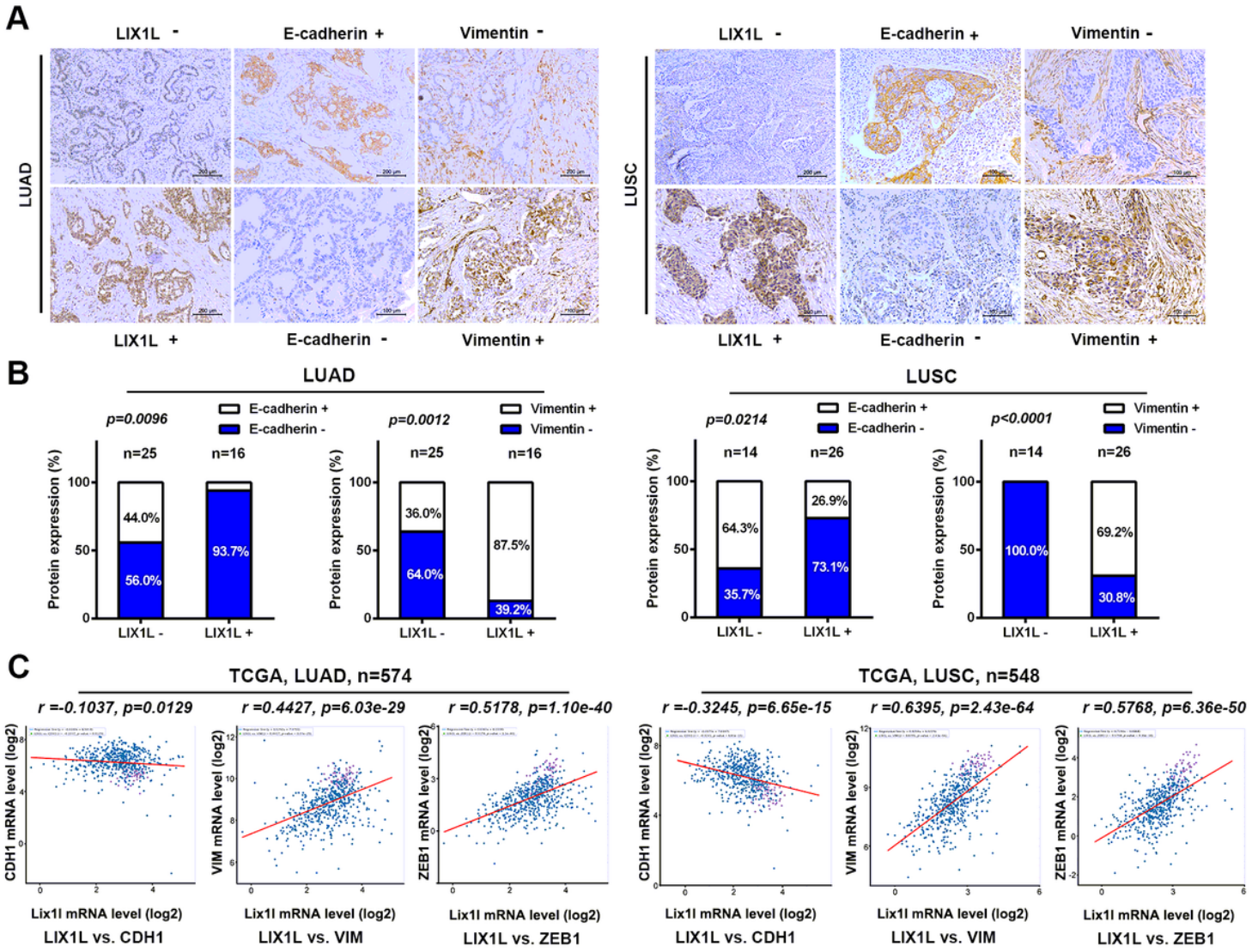

Figure 1

LIX1L expression is positively correlated with mesenchymal markers in NSCLC tumor specimens. (A) Expression of LIX1L, E-cadherin, and Vimentin protein in 81 NSCLC tissues was detected by IHC staining (Scale bar, 100 μm). **(B)** The distribution of E-cadherin or Vimentin expression in LIX1L-positive or LIX1L-negative LUAD (n=41) and LUSC (n=40) tissues was assessed by χ^2-test based on IHC results, respectively. **(C)** The correlation between LIXIL mRNA and EMT markers in LUAD (n=574) and LUSC (n=548) was evaluated by Person correlation analysis based on TCGA data.

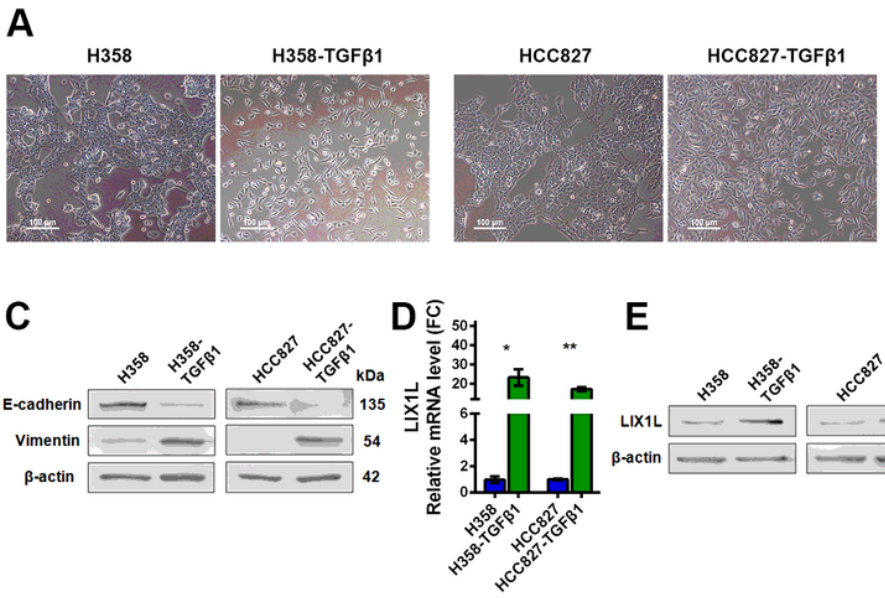

F

NSCLC cells treated with TGFβ1 VS. NSCLC cells				
	GSE49644 NCI-H358		GSE49644 NCI-HCC827	
Gene Symbol	Log FC	adj.P-value	Log FC	adj.P-value
LIX1L	2.97710117	2.35E-08	2.8519125	4.29E-07
CDH1	-3.94111061	9.31E-09	-2.94709333	3.07E-06
VIM	2.30743305	1.23E-05	2.02550697	3.11E-06

Figure 2

LIX1L expression is significantly elevated in TGFβ1-treated EMT NSCLC cells. (A) Representative morphology of H358 and HCC827 cells treated with TGFβ1 for 21 days by phase contrast microscope (Scale bar, 100μm). **(B)** EMT markers CDH1 and VIM mRNA expression were detected in TGFβ1 cells and parental cells using RT-qPCR. **(C)** E-cadherin and Vimentin protein expression was analyzed in the above cells using Western Blot assay. **(D, E)** LIX1L expression at mRNA and protein level was detected in the above cells using RT-qPCR and Western Blot assay, respectively. **(F)** LIX1L mRNA expression was analyzed in H358 and HCC827 cells treated with TGFβ1 for 48h from GEO microarray datasets GSE49644. β-actin was used as an internal control. Data were obtained from three independent experiments and shown as mean±SD. *P<0.05, ** P<0.01.

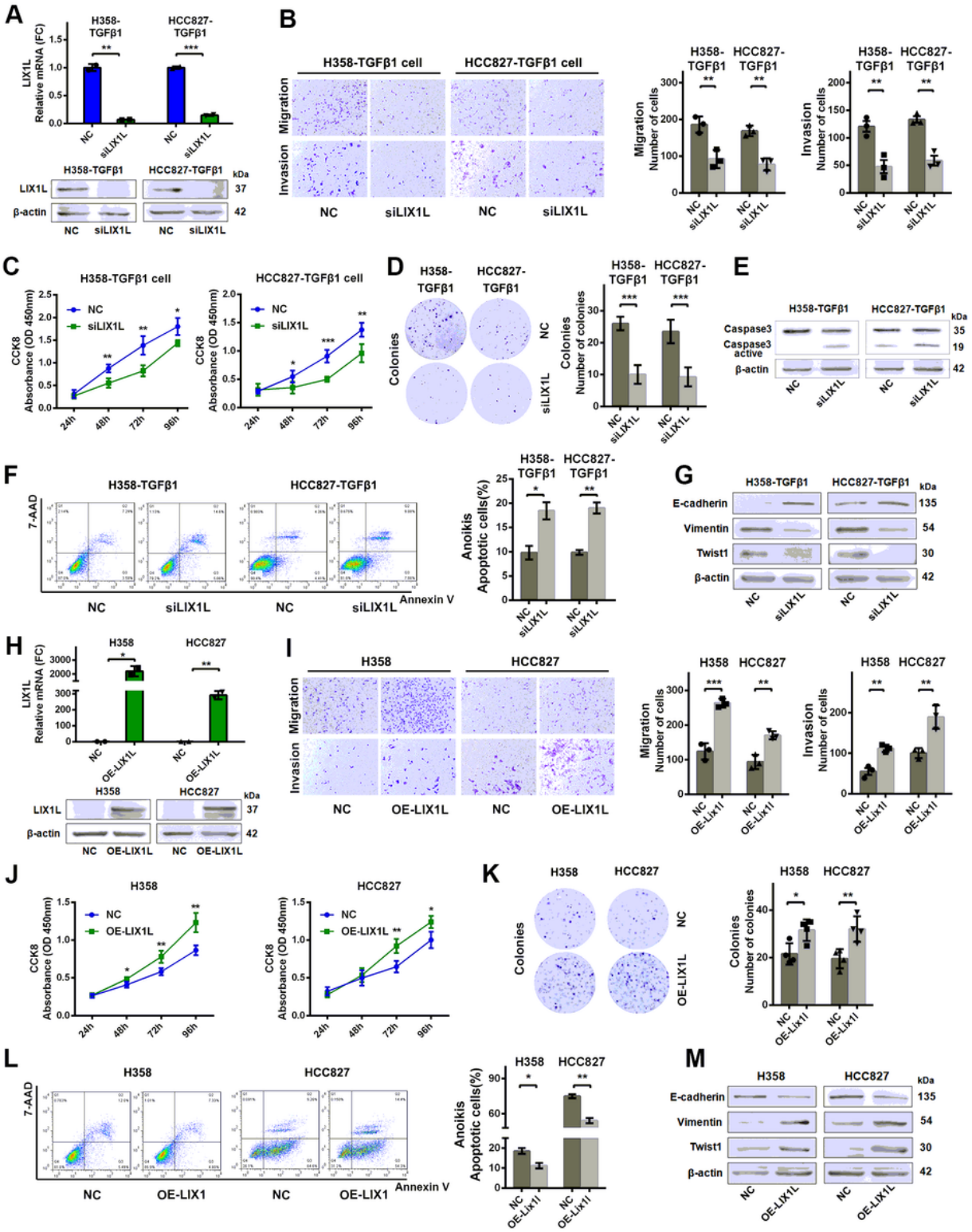

Figure 3

Upregulated LIX1L expression promotes core EMT functions of NSCLC cells. (A) RNAi was performed to knock down LIX1L expression in H358-TGFβ1 and HCC827-TGFβ1 cells. The level of mRNA or protein of LIX1L was detected by RT-qPCR (Top) and Western blot (Bottom), respectively at 48h post transfection. **(B)** Knockdown of LIX1L reduced cell migration (without Matrigel) and invasion (with Matrigel), by Transwells assay. **(C, D)** Knockdown of LIX1L reduced cell proliferation, determined by CCK8 **(C)** and

Colony formation assay **(D)**. **(E)** Knockdown of LIX1L increased the active Caspase-3 protein level in cells cultured in Poly-HEMA coated plates to induce cell anoikis. **(F)** Knockdown of LIX1L increased the apoptotic (anoikis) rate in above cells, detected by FCM with PE Annexin V-7AAD. **(G)** The EMT markers E-cadherin, Vimentin, and Twist1 protein was detected after LIX1L knockdown in TGFβ1 cells by Western blot assay. **(H)** The efficiency of LIX1L overexpression in H358 and HCC827 cells was evaluated by RT-qPCR (Top) and Western blot (Bottom), respectively at 48h post transfection. **(I)** Transwells assays were performed to detect cell migration and invasion after LIX1L overexpression. **(J, K)** Cell proliferation was detected by CCK8 and Clone formation assay, respectively. **(L)** The apoptotic (anoikis) rate was detected in LIX1L overexpression cells by FCM with PE Annexin V-7AAD. **(M)** The expression of E-cadherin, Vimentin, and Twist1 protein was detected after LIX1L overexpression in H358 and HCC827 cells by Western blot assay. *P< 0.05, ** P< 0.01, and *** P< 0.001.

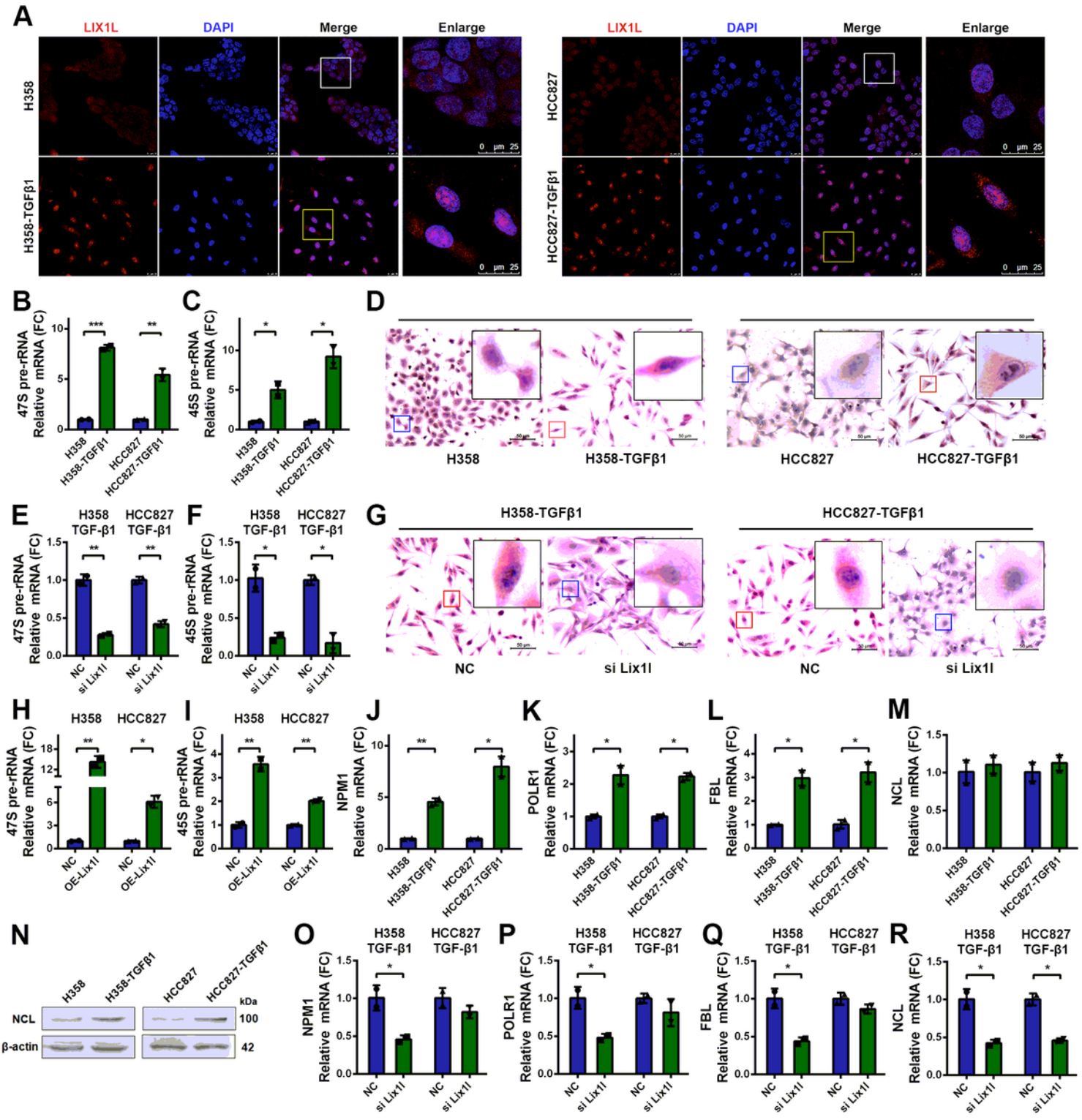

Figure 4

LIX1L is localized in the nucleoli and impacts ribosomal RNA (rRNA) synthesis in TGFβ1-treated NSCLC cells. (A) The distribution of LIX1L protein was detected in H358-TGFβ1 and HCC827-TGFβ1 cells as well as in their parental cells by Immunofluorescence (IF). **(B, C)** The levels of 47s and 45s pre-rRNA were detected in the above cells by RT-qPCR. **(D)** The nucleolar morphology was shown in the above cells by H&E staining. **(E, F)** Knockdown of LIX1L expression in TGFβ1 cells decreased the expression of 47s and

45s pre-rRNA, shown by RT-qPCR. **(G)** The nucleolar morphology was shown after LIX1L knockdown in TGFβ1 cells by H&E staining. **(H, I)** Overexpression of LIX1L expression in H358 and HCC827 cells increased the expression of 47s and 45s pre-rRNA, by RT-qPCR. **(J-M)** The POLR1, NPM1, FBL, and NCL expression in TGFβ1 cells and parental cells was assessed by RT-qPCR. **(N)** NCL protein expression in the above cells was examined by Western blot assay. **(O-R)** The POLR1, NPM1, FBL, and NCL expression was tested after LIX1L knockdown in TGFβ1 cells by RT-qPCR. **P*<0.05, ** *P*<0.01, and *** *P*<0.001.

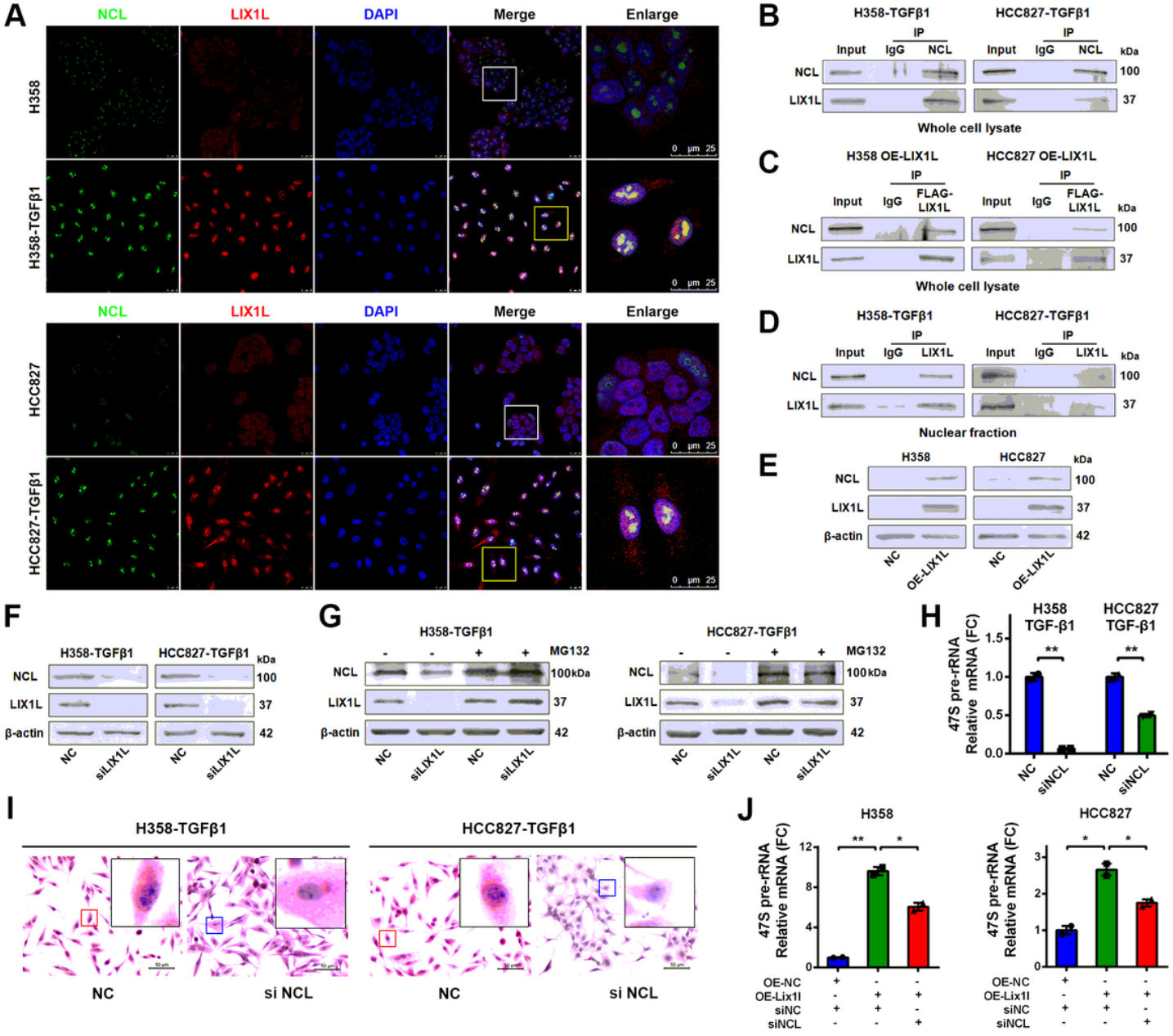

Figure 5

LIX1L interacts with NCL protein to regulate rRNA synthesis during EMT of NSCLC cells. (A) The localization of NCL and LIX1L protein was detected in H358-TGFβ1 and HCC827-TGFβ1 cells, as well as

in their parental cells, by IF. **(B)** The physical association between the endogenous LIX1L and NCL proteins was detected by Co-IP in the whole TGFβ1 cell lysate. **(C)** The physical association between the exogenously expressed Flag-LIX1L and the endogenous NCL was detected by Co-IP in the whole LIX1L-overexpression cell lysate. **(D)** LIX1L-NCL interaction was tested in the nuclear extract of TGFβ1 cells. **(E)** LIX1L overexpression increased the expression of NCL protein in H358 and HCC827 cells. **(F)** LIX1L knockdown reduced the expression of NCL protein in H358-TGFβ1 and HCC827-TGFβ1 cells. **(G)** LIX1L knockdown reduced the expression of LIX1L and NCL protein in TGFβ1 cells, but MG132 (proteasome inhibitor) treatment reversed the decrease of LIX1L and NCL protein expression. **(H)** Knockdown of NCL in H358-TGFβ1 and HCC827-TGFβ1 cells decreased the expression of 47spre-rRNA, detected by RT-qPCR. **(I)** The nucleolar morphology was detected in NCL knockdown TGFβ1 cells and control cells by H&E staining. **(J)** RT-qPCR showed that the expression of 47s pre-rRNA was increased upon LIX1L overexpression in H358 and HCC827 cells, while reversed after NCL siRNA transfection. *P<0.05 and ** P<0.01.

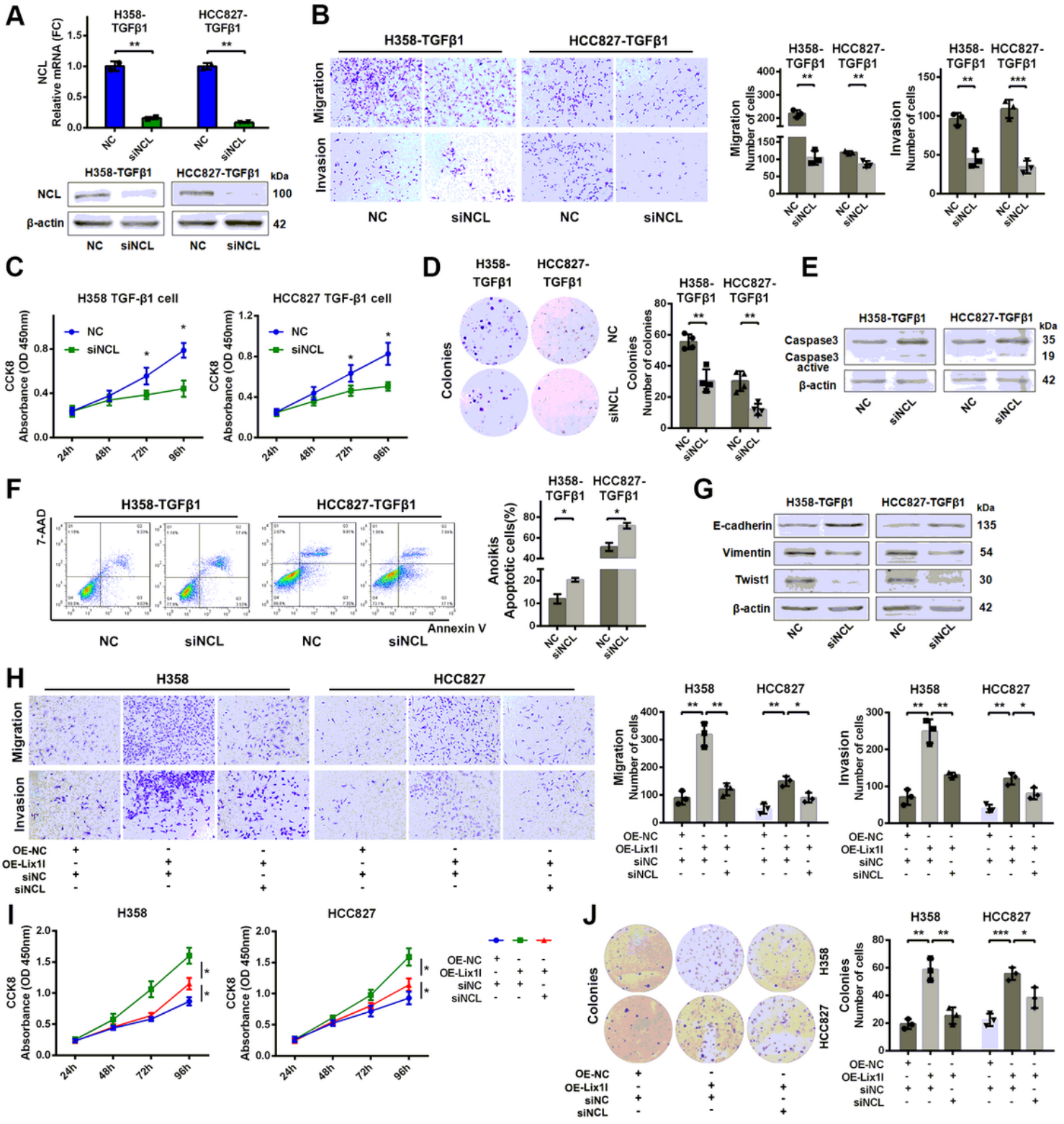

Figure 6

LIX1L-NCL promotes cell proliferation and core EMT functions of NSCLC cells. (A) The efficiency of NCL knockdown by siRNA transfection in H358-TGFβ1 and HCC827-TGFβ1 cells was showed by RT-qPCR (Top) and Western blot (Bottom), respectively at 48h post transfection. **(B)** Knockdown of NCL reduced cell migration (without Matrigel) and invasion (with Matrigel) in TGFβ1 cells. Knockdown of NCL reduced proliferation **(C, D)**, and anoikis resistance **(E, F)**. **(G)** The expression of E-cadherin, Vimentin and Twist1

was detected after NCL knockdown in TGFβ1 cells by Western blot assay. **(H)** Transwells assay showed that knockdown NCL expression reversed the increase of migration and invasion due to LIX1L overexpression in H358 and HCC827 cells. **(I, J)** CCK8 and clone formation assay indicated that NCL knockdown abrogated the enhanced proliferation activity induced by LIX1L overexpression in H358 and HCC827 cells. **P*<0.05, ** *P*<0.01, and *** *P*<0.001.

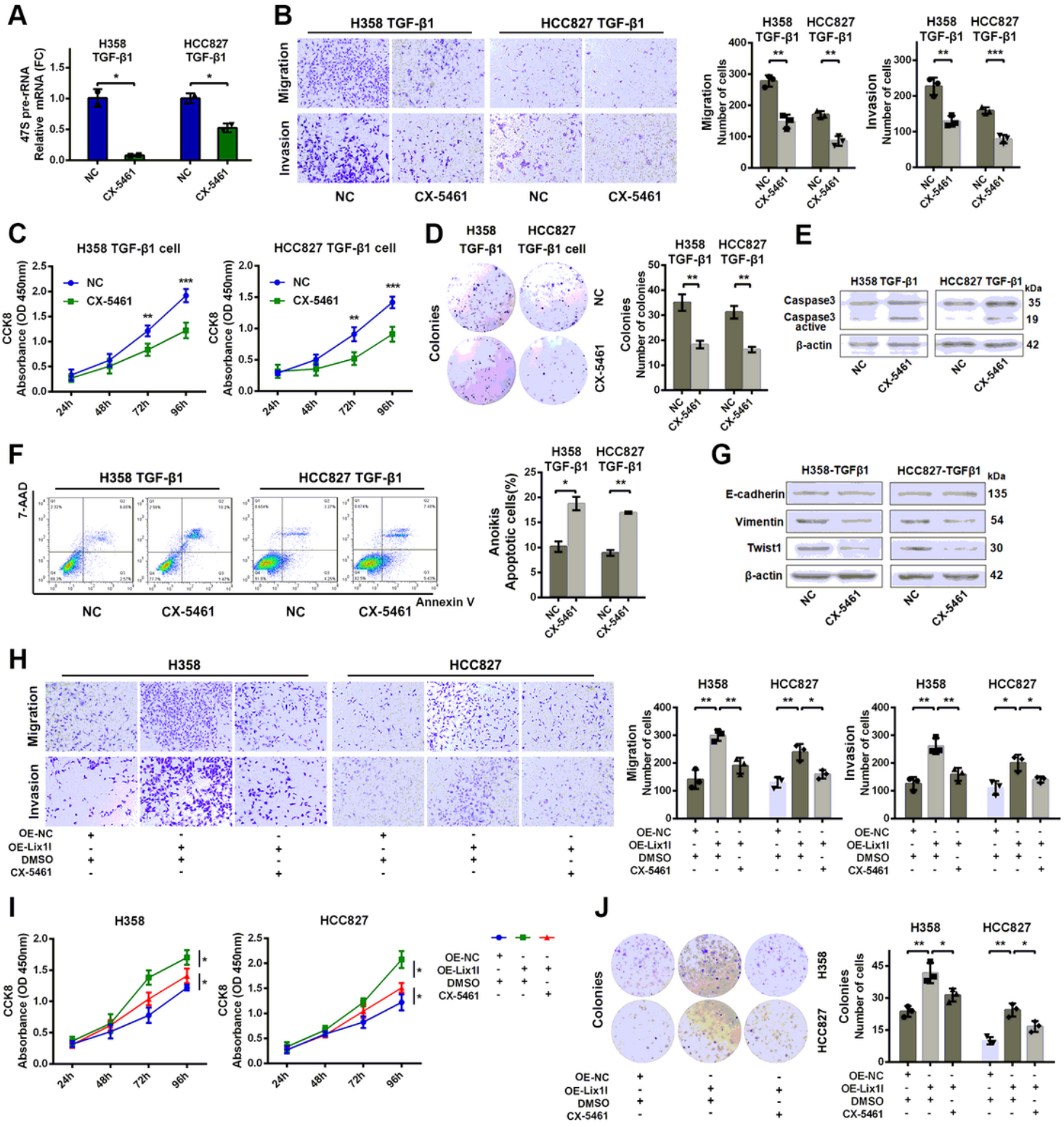

Figure 7

rRNA synthesis participated in LIX1L-mediated cell proliferation and core EMT functions of NSCLC cells. **(A)**The level of 47s pre-rRNA was detected in H358-TGFβ1 and HCC827-TGFβ1 cells treated with rRNA synthesis inhibitor CX-5461 by RT-qPCR assay. **(B)** The effects of CX-5461 treatment on cell migration and invasion were detected in the above cells by Transwells assay. **(C, D)** The effects of CX-5461 treatment on cell proliferation were detected in the above cells by CCK8 and clone formation assay, respectively. **(E, F)** The impact of CX-5461 treatment on cell anoikis resistance ability was assessed by Western Blot (active Caspase-3 protein) and FCM (PE Annexin V-7AAD apoptotic assay) in H358-TGFβ1 and HCC827-TGFβ1 cells cultured in Poly-HEMA coated plates to induce cell anoikis. **(G)** The effects of CX-5461 treatment on the expression of E-cadherin, Vimentin and Twist1were examined by Western blot assay. **(H)** Transwells showed that CX-5461 treatment abrogated the increase of migration and invasion ability due to LIX1L overexpression in H358 and HCC827 cells. **(I, J)** CCK8 and clone formation assay indicated that CX-5461 treatment reversed the cell proliferation activity induced by LIX1L overexpression in H358 and HCC827 cells, respectively. *P<0.05, ** P<0.01, and *** P<0.001.

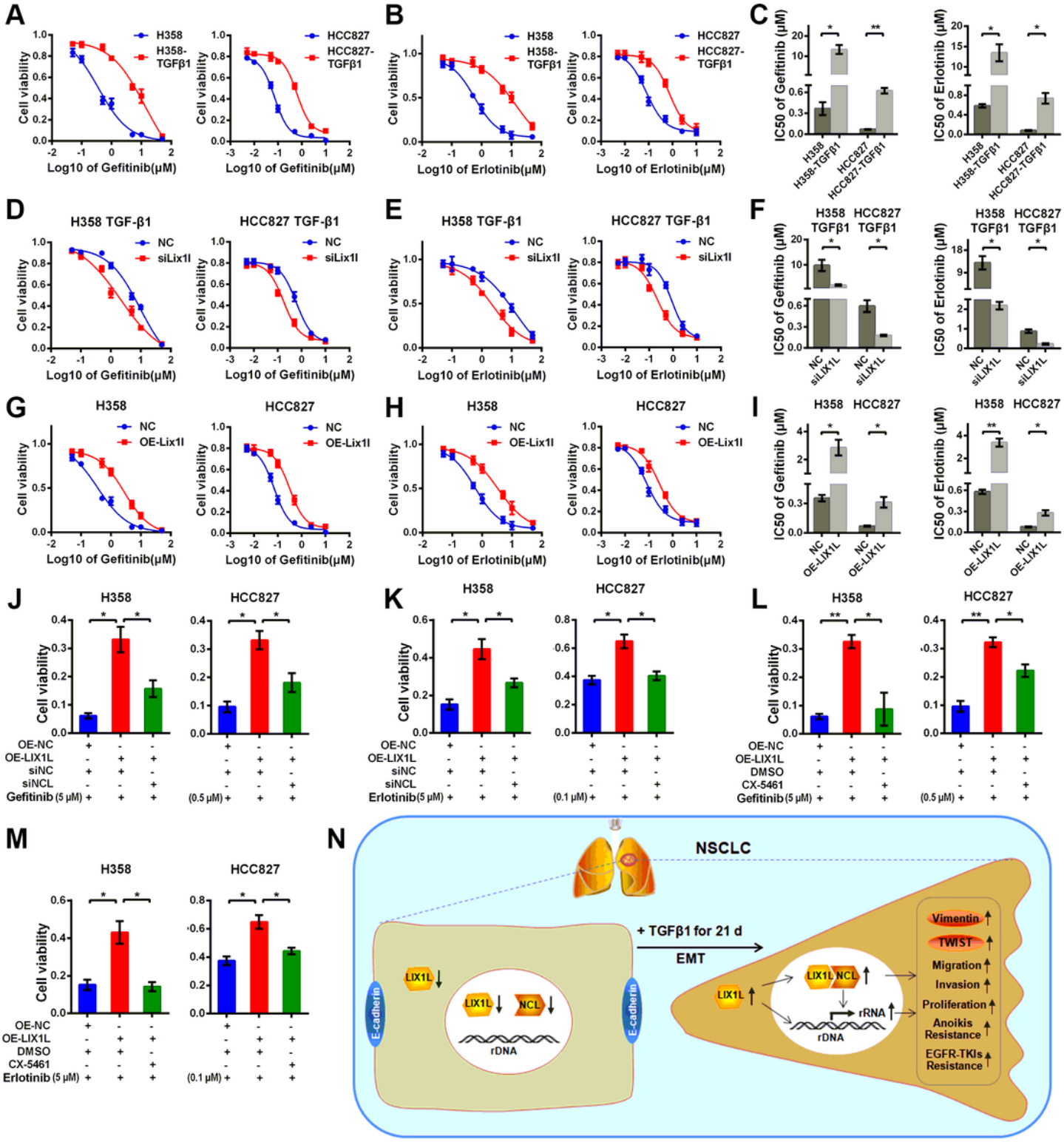

Figure 8

Upregulated LIX1L enhances EGFR-TKIs resistance of TGFβ1-treated EMT NSCLC cells in part by upregulating NCL expression and rRNA synthesis. (A, B) Cell viability was assessed by CCK8 assays in TGFβ1 and parental cells upon the indicated doses of gefitinib or erlotinib treatment. **(C)** The IC_{50} value was assessed based on the above CCK8 results. **(D, E)** H358-TGFβ1 and HCC827-TGFβ1 cells were transfected with NC or LIX1L siRNA for 24h and then treated with the indicated doses of gefitinib or

erlotinib, respectively. The cell viability was assessed by CCK8 assays. **(F)** The IC_{50} value was assessed based on the CCK8 results as in D and E. **(G, H)** H358 and HCC827 cells were transfected with an empty vector or LIX1L-vector for 24h and then treated with the indicated doses of gefitinib or erlotinib, respectively. The cell viability was assessed by CCK8 assays. **(I)** The IC_{50} value was assessed based on the CCK8 results as in G and H. CCK8 assays showed that the cell viability upon gefitinib or erlotinib treatment was increased by LIX1L overexpression in H358 and HCC827 cells, while it was in part abrogated by NCL knockdown **(J, K)**, and by CX-5461 treatment **(L, M)**. **(N)** Schematic model illustrating the mechanisms by which LIX1L-mediated EMT and EGFR-TKIs resistance in NSCLC cells. *P<0.05 and ** P<0.01.

Supplementary Files

This is a list of supplementary files associated with this preprint. Click to download.

- SupplementalfileUncroppedWesternblot.docx
- SupplementaryFiguresandLegends.docx
- SupplementaryTables.xlsx